

# Catalytic nanomotors: fabrication, mechanism, and applications

John GIBBS (✉) and Yiping ZHAO

Nanoscale Science and Engineering Center, Department of Physics and Astronomy, The University of Georgia, Athens, GA 30602, USA

© Higher Education Press and Springer-Verlag Berlin Heidelberg 2011

**ABSTRACT:** Catalytic nanomotors are nano-to-micrometer-sized actuators that carry an on-board catalyst and convert local chemical fuel in solution into mechanical work. The location of this catalyst as well as the geometry of the structure dictate the swimming behaviors exhibited. The nanomotors can occur naturally in organic molecules, combine natural and artificial parts to form hybrid nanomotors or be purely artificial. Fabrication techniques consist of template directed electroplating, lithography, physical vapor deposition, and other advanced growth methods. Various physical and chemical propulsion mechanisms have been proposed to explain the motion behaviors including diffusiophoresis, bubble propulsion, interfacial tension gradients, and self-electrophoresis. The control and manipulation based upon external fields, catalytic alloys, and motion control through thermal modulation are discussed as well. Catalytic nanomotors represent an exciting technological challenge with the end goal being practical functional nanomachines that can perform a variety of tasks at the nanoscale.

**KEYWORDS:** nanomotors, catalysis, glancing angle deposition (GLAD), bubble propulsion, self-electrophoresis

## 1 Introduction

Recent advances in the field of catalytic nanomotors which are capable of moving autonomously constitute a major step forward to develop practicable functional nanomachines. Designing and powering inorganic micro and nano scale motors represent tremendous challenges and exciting opportunities for researchers [1]. The promise for great technological advances in the field of nanotechnology through controlled motion of nanomotors has recently brought significant attention to this field; controlled drug delivery and other forms of nanomedicine, mobile sensors, self-assembled complex nanoarchitectures, and advanced forms of micro and nano electronics are possible examples

of subfields that may greatly benefit from this research [1–7]. Clearly, mobility and control of motion of nanomachines and nanoactuators will have drastic consequences on future technologies, and applications yet unimagined are possible rendering this research as a merited investment.

Although the nanotechnology community is embracing this new endeavor, numerous challenges still remain before functional nanomachines are realized. Besides the obvious difficulty of manufacturing such small devices, other major difficulties exist such as how to control their motion and how they can be efficiently powered [2–7]. Researchers from a multitude of institutions and scientific backgrounds have begun tackling these tough questions, and the amount of interest in the field over the past 15 years has increasingly gained momentum as can be seen by the number of publications over this span of time [7]. In this

review, we summarize the evolution of this field and the multitude of avenues traversed by the participating groups. Although nanomotors mobilized by several energy sources exist, here we focus upon the chemically-fueled autonomous catalytic nanomotor which is an analog of naturally occurring protein motors found in biologic systems.

### 1.1 Natural nanomotors

The chemically-powered motor protein classes, myosins, kinesins and dyneins, perform a wide variety of essential cellular functions in biology such as organelle and vesicle transport [8]. All three of these molecular motors use adenosine triphosphate (ATP) as a chemical fuel for the conversion of chemical energy into mechanical work; chemical energy is stored in the ATP molecule by the three closely oriented negatively charged phosphate tails endowing the molecule with a high energy configuration, and as ATP is hydrolyzed to adenosine diphosphate (ADP), which often can be further hydrolyzed to adenosine monophosphate (AMP), free energy from the closely packed phosphate tails is released and is available to do work [9]. The energy exchange allowing for the conversion of food energy for an organism into both catabolic and anabolic forms of metabolism is regulated by ATP, and through this process, cell metabolism is possible.

As an example, skeletal muscle contraction arises by the ATP-powered shortening of myosin filament along a passive filament of actin [10]. A skeletal muscle fiber consists of repeating sections of myosins and actins allowing for the macro-scale movement of large muscles. During muscle contraction, the ATP causes a conformational change in the myosin motor which induces a net movement of the two filaments with respect to one another. To illustrate this example, Kron and Spudich performed an experiment to test the ATP concentration dependence upon movement of actin filaments across myosin fixed to a glass surface [11]. Figure 1(a) shows the migration of actin filaments over the myosin-immobilized surface over a 38 s interval, and Fig. 1(b) shows the dependence of ATP concentration on speed of the actin filaments across the surface [11]. As the concentration of ATP increases, the speed of the actin filament increases until a limiting concentration is reached. The active myosin responds to the presence of a chemical fuel converting the chemical energy into kinetic energy. This example shows the importance of chemically-powered molecular motors in the field of biology and how the actuation of nanomotors with locally available fuel is possible. Researchers hope to

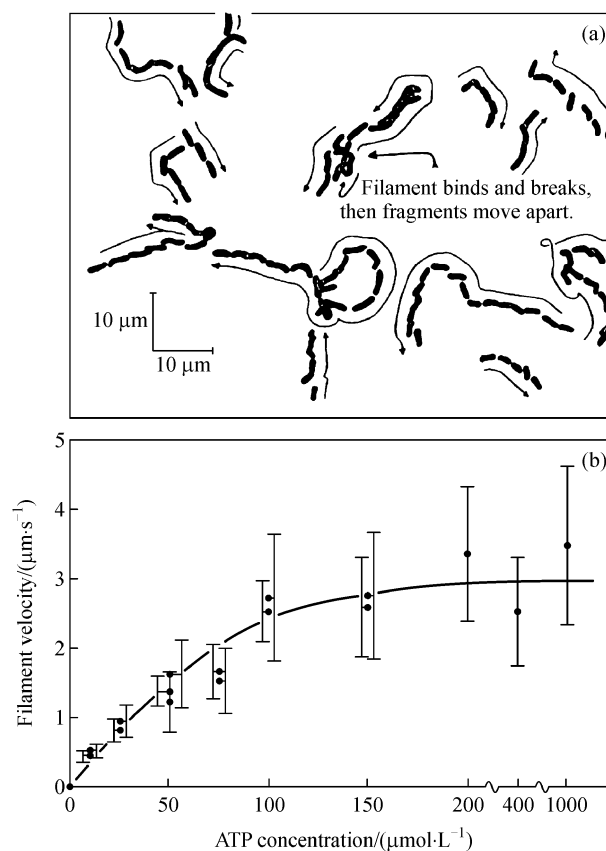


**Fig. 1** (a) Over a 38 s interval, actin filaments migrate across the myosin-immobilized surface; (b) Filament velocity versus ATP concentration; speed initially increases with ATP concentration and eventually plateaus around 200  $\mu\text{mol}/\text{L}$ . (Reproduced with permission from Ref. [11], Copyright 1986 The National Academy of Sciences of the United States of America)

emulate the secrets of biology in order to fabricate artificial motors to perform tasks similar to naturally occurring motors or even to develop applications not seen in nature.

### 1.2 Hybrid nanomotors

Billions of years of evolution have allowed for the design perfection of naturally occurring motors and therefore they perform well defined and controlled behaviors. The most practical method researchers use to design functional artificial motors is to make use of readily available motor structures from nature [12–14]. By combining naturally occurring components to artificially fabricated structures, hybrid nanomotors were made possible. As an example, the transportation of inorganic cargo was shown to be possible through the catalysis of actin filament polymerization [15]. In this study, 0.5  $\mu\text{m}$  ActA-coated polystyrene beads were propelled in an actin environment with an average velocity of 0.1–0.15  $\mu\text{m}/\text{s}$ . Figure 2 shows an

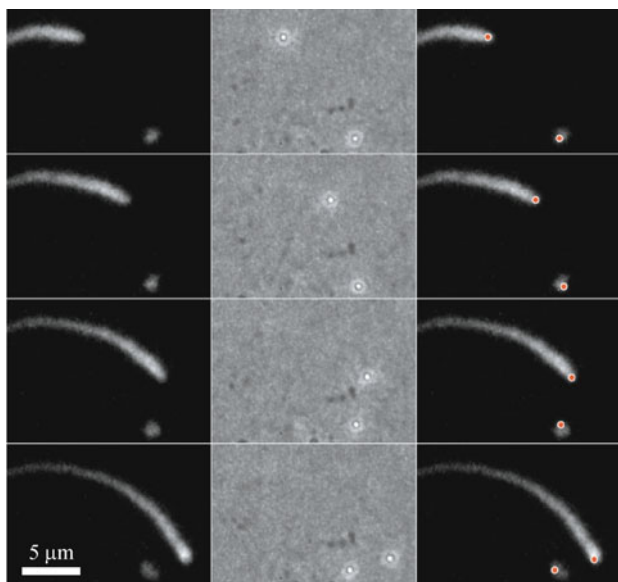


**Fig. 2** Left column: fluorescent rotamine-actin comet tail for a directional bead and a stationary bead; Middle column: micrograph of the two beads; Right column: bead positions superimposed on fluorescent images. (Reproduced with permission from Ref. [15], Copyright 1999 The National Academy of Sciences of the United States of America)

active and a stationary microbead in 4 movie frames separated by 30 s. The “comet tail” arises from fluorescence imaging and shows the location of the rotamine-actin showing the trajectory of the bead. Another interesting example is a rotary structure that combines a metal nanorod that is the “propeller” attached to a biomolecular motor that spins the propeller. Figure 3 shows how the Ni propeller and the  $F_1$ -ATPase biomolecular motor are combined using various attachment chemistries; the propeller is in this case fueled by ATP [16]. These two examples show the practical fabrication of combined artificial and natural parts; the next natural step was to design purely artificial catalytic nanomotors.

### 1.3 Manmade catalytic nanomotors

The term catalytic nanomotor refers to inorganic structures that use a chemical to gain mobility via an onboard catalyst. In this manner, they are analogs of naturally occurring bionanomotors which utilize energy obtained from the environment to do work and are ubiquitous in nature. The most commonly used chemical fuel is hydrogen peroxide  $H_2O_2$ . Hydrogen peroxide spontaneously decomposes into water and oxygen,  $H_2O_2 \rightarrow 2H_2O + O_2$ , but at a very slow rate. A catalyst can greatly increase the reaction rate, and most of the transition metals

catalyze this reaction. Since a large amount of energy is available as the  $H_2O_2$  decomposes, catalytic nanomotors are able to gain mobility by carrying an onboard catalyst. Although  $H_2O_2$  is generally the most commonly used source of energy, other chemical fuels that are more bio-compatible such as glucose have been used as well [17–19].

Just as natural biomotors have specific functions based upon their physical and chemical specifications, catalytic nanomotors exhibit various behaviors based upon their compositions and physical dimensions. A commonality between fabrication methods is the asymmetric distribution of the catalyst as the asymmetry allows for directional movement. Several design techniques and explanations of the underlying physics exist in the literature, and at present, both contradictions and agreements exist about how these motors operate [20]. Recent research suggests that the discrepancies over the propulsion mechanisms may be due to the types of materials used for fabrication, and although researchers are getting ever closer to understanding this mechanism, there are still some unexplained phenomena. Here we summarize the types of nanomotors studied, their possible driving mechanisms, and the current status of this field.

## 2 Fabrication

A major challenge in catalytic nanomotor research is the fabrication of such small devices. Researchers generally agree that a necessary feature of a catalytic nanomotor is to distribute an onboard catalyst asymmetrically on a nanostructured backbone. Therefore, design and fabrication must take this necessity into account, and as will be discussed in the following sections, the types of the backbone materials used as well as the physical shape of the motors dictates the types of motions that are observed. Here we will focus upon the two main methods for catalytic nanomotor fabrication: template directed electroplating (TDEP) and physical vapor deposition (PVD); both methods are effective for fabricating catalytic nanomotors with different structural materials and asymmetrically distributed catalysts. Also discussed are combinations of the techniques which also fall under one or both of these categories.

### 2.1 Template directed electroplating

Nanorod nanomotors with sections of various metals can

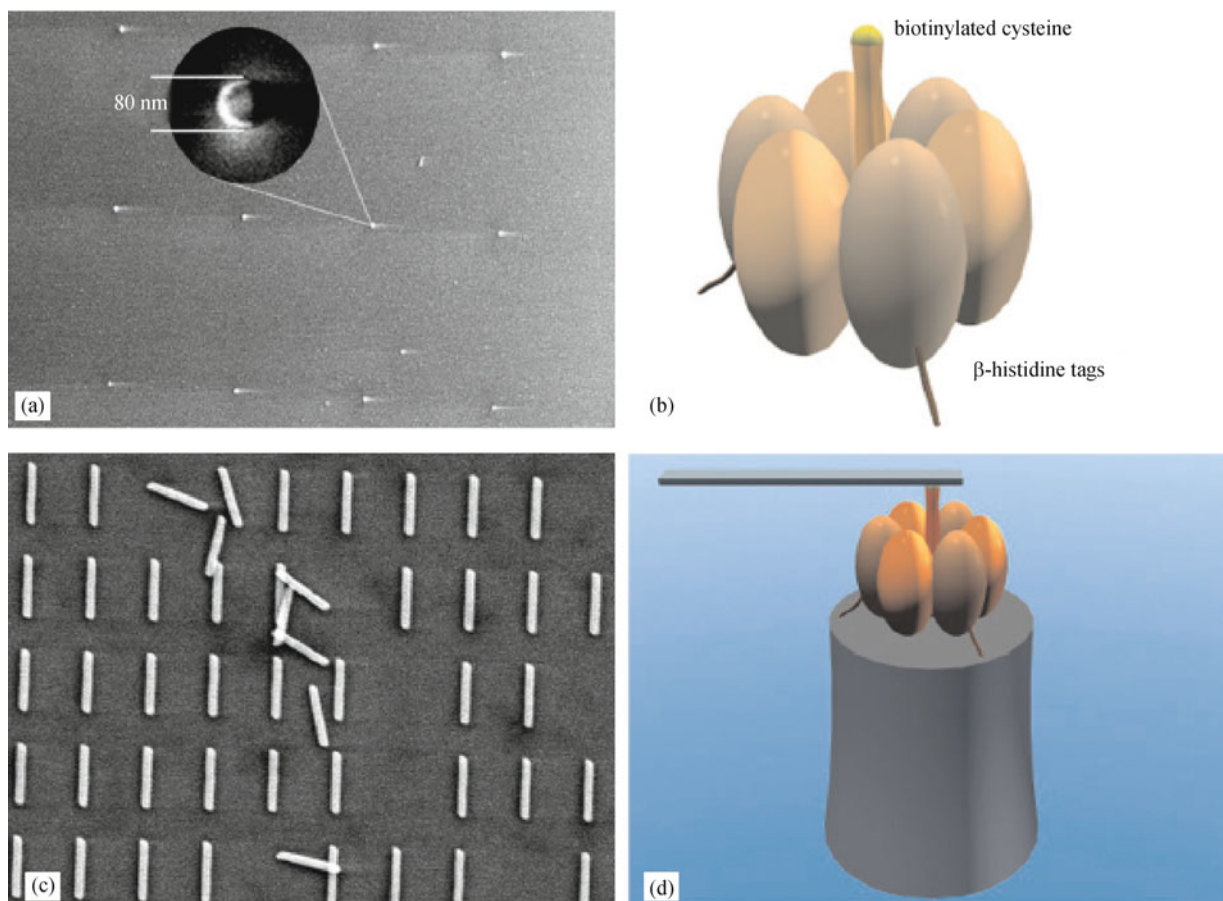


**Fig. 3** (a)(c) Ni nanorod rotors; (b)  $F_1$ -ATPase biomolecular motor; (d) Schematic of the combined architecture. (Reproduced with permission from Ref. [16], Copyright 2000 American Association for the Advancement of Science)

be fabricated using electrochemistry combined with template growth. The fabrication of metallic barcode nanorods by template directed electroplating (TDEP) was first shown by Natan et al. [21]. In this study, a porous  $Al_2O_3$  membrane with uniformly sized pores is used as a template for the electrochemical deposition of an array of metallic nanorods which can be released from the template. As shown in Fig. 4, the fabrication process of multi-metal nanorods consists of Ag evaporation onto the membrane, followed by an electrochemical deposition of an Ag film, Au and Ag are then electrodeposited into the pores of the membrane, and finally the Ag film and  $Al_2O_3$  membrane are dissolved to release the nanorods. Since it is necessary to have multiple materials to fabricate catalytic nanomotors, TDEP is an appropriate method since it allows a single structure to consist of multiple metals.

For catalytic nanomotors, the asymmetric distribution of the catalyst is necessary for directed movement as will be discussed. The catalyst layer is easily placed on one end of the nanorod by adding multiple layers to the nanorod

structure so that this asymmetry exists. Mallouk and Sen fabricated autonomous Au/Pt striped nanorods using the TDEP method, shown in Fig. 5(a), in which the Pt catalyzes the decomposition of  $H_2O_2$ . They hypothesized that the interfacial tension created by the oxygen reaction product was the cause of the movement as will be discussed in the propulsion mechanism section [22]. Ozin et al. fabricated Au-Ni nanorotors using TDEP as well; in this study, the Ni acts as the catalyst for the decomposition of  $H_2O_2$ , and when the Au end of the nanorod becomes tethered to the surface of the microscope slide, the nanorotors spins about the tether point with the Ni end propelling the rotor shown in Fig. 5(b) [1]. This method was also used for fabricating alloys for increasing nanomotor speed [23] and electroplating not only along the axis of the rod, but along one face as well [24]. Template electroplating has been used without  $Al_2O_3$  membranes to fabricate tubular microengines as seen in Fig. 5(c) [25], and another example shown in Fig. 5(d) uses a template made with lithography to fabricate a rotating

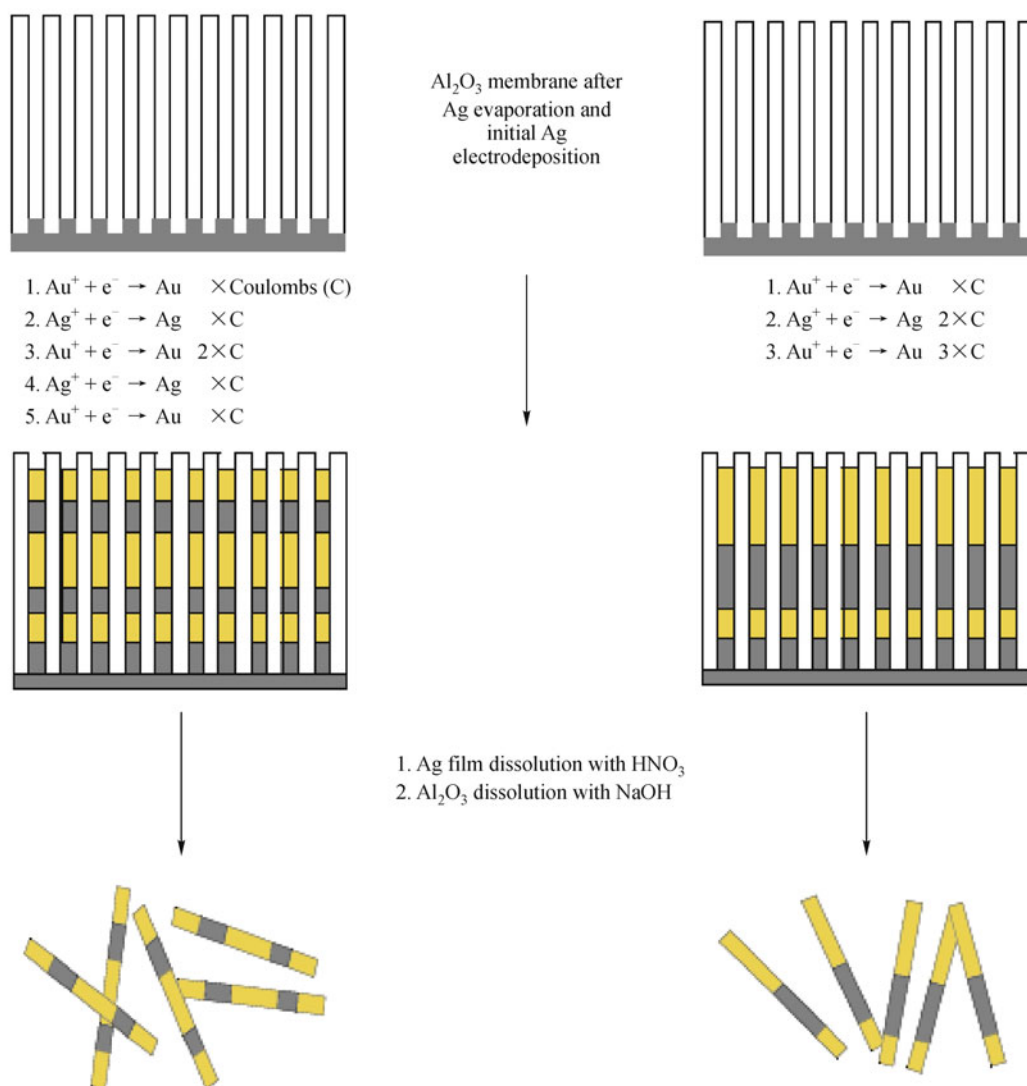


**Fig. 4** Fabrication process of template directed electroplating. First Ag is evaporated onto the Al<sub>2</sub>O<sub>3</sub> porous membrane and an Ag is electrodeposited onto this film; Au and Ag are deposited into the pores, then the Ag film and the membrane are dissolved releasing the nanorods. (Reproduced with permission from Ref. [21], Copyright 2001 American Association for the Advancement of Science)

gear structure [26]. TDEP also allows for the addition of multiple layers to increase control such as by adding a ferromagnetic material into the rod to control the direction of swimming [27]. Mirkin et al. combined both TDEP and physical vapor deposition to design catalytically driven nanorotors as well [24]. TDEP is an effective and popular way to produce a large number of nanorod nanomotors with multiple metals that are roughly uniform in shape.

## 2.2 Physical vapor deposition

Physical vapor deposition (PVD) has been shown to be an effective and useful catalytic nanomotor fabrication method, and is becoming more prevalent in this field. PVD

is an easy and cost-effective method that consists of coating substrates by the heating and evaporation of metals and metal-oxides. Some advantages over TDEP exist such as the ability to deposit a wider range of materials, the process takes far fewer steps, and by combining PVD with substrate manipulation, a greater spectrum of geometries with asymmetric catalyst distributions are possible.

The simplest form of PVD is the deposition of a thin film onto a substrate. In this case, the substrate is placed directly above the source material at a 0° vapor incidence angle (the vapor direction is parallel to the substrate surface normal) and is coated with a film of the evaporated material. Using PVD in this case, a very simple catalytic nanomotor can be fabricated by coating a catalyst layer onto a structure that is

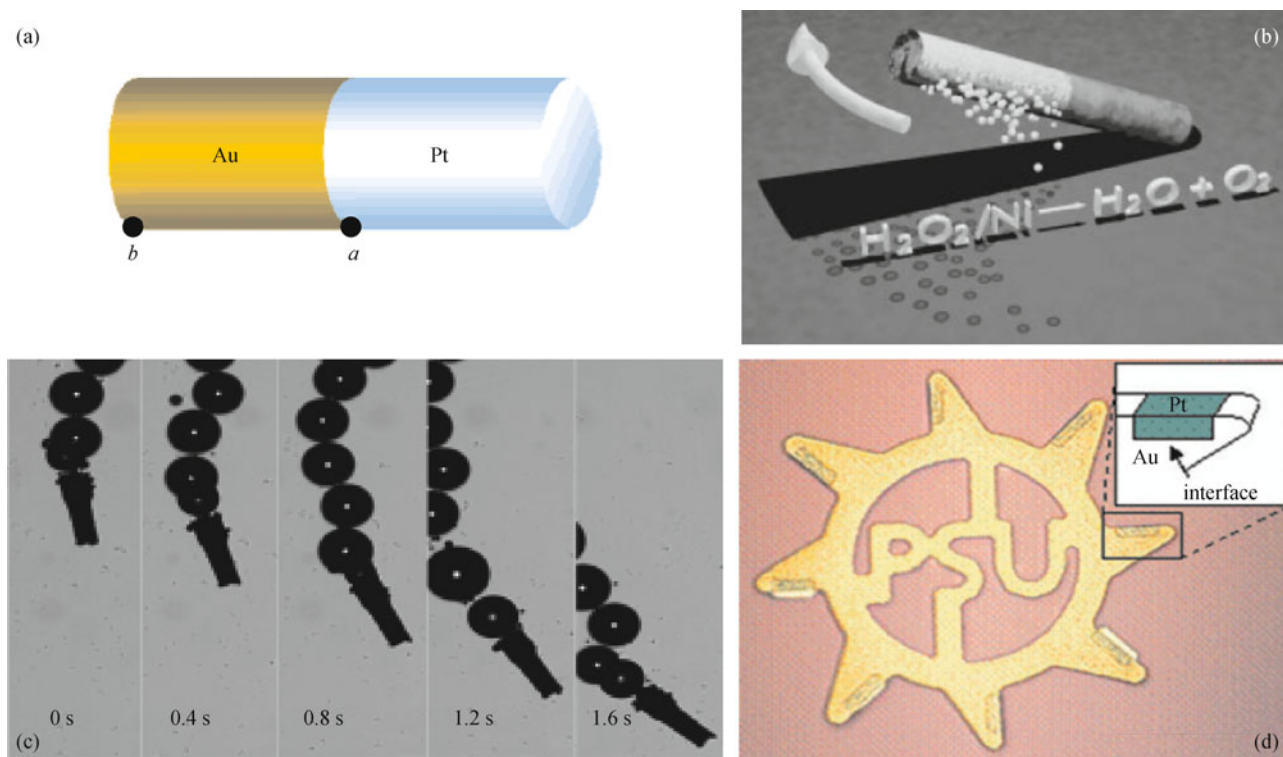


**Fig. 5** Examples of template directed electrodeposition-grown nanomotors: **(a)** schematic of a Pt-Au striped nanorod nanomotor (Reproduced with permission from Ref. [22], Copyright 2004 American Chemical Society); **(b)** Ni-Au nanorotor (Reproduced with permission from Ref. [1], Copyright 2005 WILEY-VCH Verlag GmbH & Co. KGaA, Weinheim); **(c)** micrograph of tubular microengines (Reproduced with permission from Ref. [25], Copyright 2010 American Chemical Society); **(d)** lithography template rotary gear (Reproduced with permission from Ref. [26], Copyright 2005 WILEY-VCH Verlag GmbH & Co. KGaA, Weinheim).

first deposited onto the substrate. The half-coating of submicron silica spheres with a metal was demonstrated by Whitesides et al. [28]. The so-called Janus sphere consists of two hemispheres with differing materials. If one of these two materials was a catalyst, then directed propulsion was hypothesized to ensue in the presence of fuel [29]. Experimental verification of active motion was demonstrated first by using Pt-coated polystyrene microspheres [30] and later using Pt-coated silica microspheres shown in Fig. 6 [31]. A Janus sphere with one side Au and the other Pt was fabricated as well [32], and another example consists of a microsphere with various overlapping sections of Au and Pt in which the exposed Au area determines the nanomotor motion behaviors [33]. Clearly, other structures besides spheres can be coated in a similar manner; Au-Ru bimetallic nanorods fabricated by TDEP were distributed onto a substrate and modified by PVD thin film depositions of Cr, SiO<sub>2</sub>, Pt, and Au to make fast micro-rotors [34]. Thin film PVD combined with circular or square patterned photoresists resulted in catalytic microtube jet engines capable of reaching speeds of ~ 2 mm/s [35].

By tilting the substrate to a large angle (> 80°) during

vapor deposition, an array of nanostructures grows on the surface of the substrate. This technique is known as dynamic shadowing growth (DSG) and is an effective method for growing complex nanomotor geometries [36–39]. By manipulating the substrate during the deposition, a variety of structures can be achieved. After nanostructure growth, the individual micro or nanostructures can be removed from the surface and suspended. He et al. demonstrated the fabrication of rotary nanorods, rotary L-shaped structures, and rolling spiral nanomotors [40]. Figure 7 shows the step-by-step process of the growth of an L-shaped Si nanomotor. In the first step (top of Fig. 7), the Si source material is deposited at a large angle  $\theta$ ; next the substrate is rotated 180° azimuthally and another deposition of Si follows so that the angle of growth is in the opposite direction; and lastly, to deposit the Pt catalyst, a thin film of Pt is deposited at a small angle. The resulting structure is L-shaped with asymmetrically distributed Pt on the long arm.

DSG has been used to fabricate multi-constituent structures as well. By starting with a monolayer of silica microbeads on a Si substrate and depositing an oxide layer

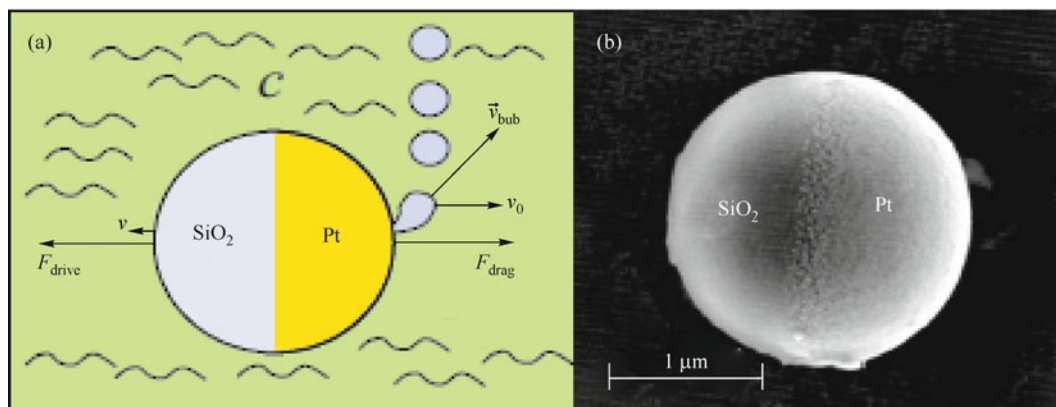


**Fig. 6** (a) Schematic of the Pt-coated silica microsphere; (b) A SEM image showing the same structure. (Reproduced with permission from Ref. [31], Copyright 2009 American Institute of Physics)

onto the monolayer at a large angle, the resulting structure consists of a spherical microbead head with an oxide arm. Figure 8 shows the fabrication process of a rotary structure [41]. Figure 8(a) shows an optical micrograph of a partial monolayer of  $2.01 \mu\text{m}$  silica microbeads. In Fig. 8(b), the substrate containing the microbead monolayer is tilted to a large angle, and a layer of  $\text{TiO}_2$  is deposited followed by a thin film of Pt deposited after the substrate is rotated back to a small angle shown in Fig. 8(c). Figure 8(d) shows an SEM of the resulting structure with the silica microbead head and the oxide arm with a layer of Pt acting as the catalyst. When placed into a solution of  $\text{H}_2\text{O}_2$  this structure rotates about an axis defined by the center of the microbead. These structures exhibit very similar rotation rates and have practically identical structural morphologies. The DSG fabrication process is an effective way to produce a large number of similar structures and is a simple and cost effective method.

### 2.3 Advanced assemblages

The template-directed electroplating and physical vapor deposition techniques described above are effective methods for producing individual nanomotors, but to manufacture more complex geometries, self-assembly techniques must be utilized. The engineering of structures with multiple individual parts is a particularly difficult challenge. Initial attempts have been made to assemble multiple parts to fabricate complex nanomotor structures, and this challenge represents the next step in nanomotor research and engineering.

Assemblages of macroscopic catalytically driven PDMS plates were shown to organize themselves more rapidly due to the active motion resulting from the catalyze reaction of

the Pt section [42]. These aggregates are described to organize themselves based on altering hydrophobic and hydrophilic sections of the plates. Flexible hinged nanorods were achieved by electrodepositing a nanorod consisting of 3 sections: Pt-Au-Pt [43]. The rods were then encapsulated by a polymer and the Au section was then etched leaving the two Pt sections attached but separated by flexible material. Using magnetically-navigation and oppositely charged polymers, Sen et al. was able to direct a nanorod nanomotor to a spherical cargo, pick up the cargo, and move it [44]. Sphere dimers consisting of Pt and  $\text{SiO}_2$  microspheres were also fabricated by depositing a half sphere of Pt onto the microbeads and annealing them in at  $900^\circ\text{C}$  [45]. The annealing process causes the Pt to become approximately spherical but remain attached to the microbead. A schematic of the fabrication process can be seen in Fig. 9. Doublets of self-propelled Janus spheres [46] as well as interacting spinning nanorods have been studied as well [34]. By magnetizing structures with ferromagnetic material grown by DSG, assemblages of various structures were also achieved [47].

## 3 Propulsion mechanisms

The various reports in the literature lead to the conclusion that several different underlying propulsion mechanisms may exist to describe nanomotor motion. A review of the various examples that exist can be found in Ref. [20]. The major discrepancy involves the direction of motion for a catalytic nanomotor. Both conclusive evidences for the movement toward the catalyst [48] as well as away from the catalyst have been observed [40–41]. Two possible mechanisms have been proposed to describe motion away

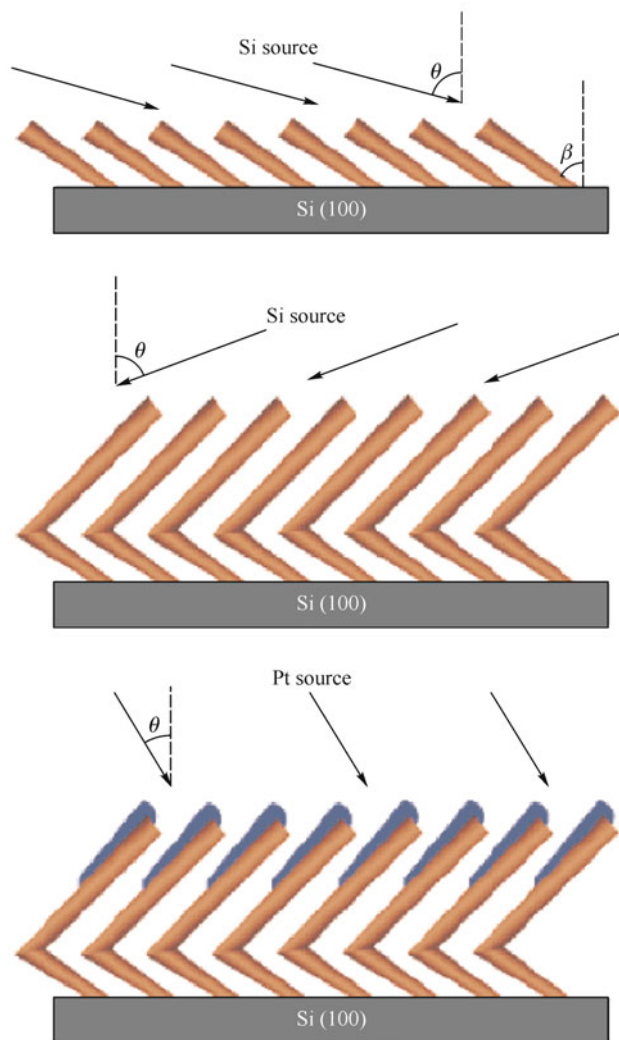


**Fig. 7** Schematic of the fabrication process for a DSG-grown L-shaped nanorod nanomotor. The Si backbone is grown at a large angle  $\theta$  after which the substrate is rotated azimuthally  $180^\circ$  and another deposition of Si nanorod follows. The substrate is then rotated in a polar manner back to a small angle at which the Pt catalyst is deposited. (Reproduced with permission from Ref. [40], Copyright 2007 American Chemical Society)

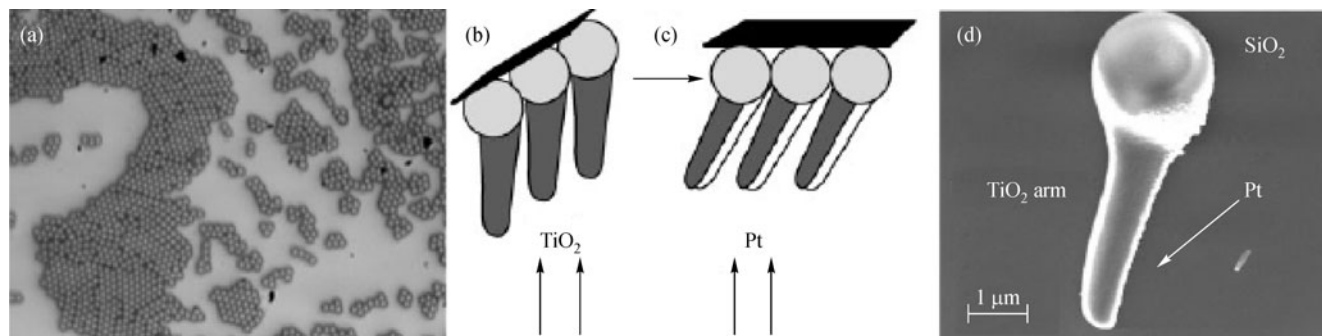


**Fig. 8** (a) A micrograph of a sub-monolayer of  $\text{SiO}_2$  microbeads on a Si substrate; (b)  $\text{TiO}_2$  is deposited at a large angle to grow oxide arms; (c) The Pt catalyst is deposited at a small angle; (d) Example SEM image of an individual nanomotor structure showing the multiple parts. (Reproduced with permission from Ref. [41], Copyright 2009 WILEY-VCH Verlag GmbH & Co. KGaA, Weinheim)

from the catalyst site: diffusiophoresis and bubble propulsion, and two have been proposed for motion toward the catalyst: interfacial tension gradients and self-electrophoresis.

### 3.1 Diffusiophoresis

The asymmetry of a catalytic nanomotor plays an important role in the description of motion. When the catalyst is distributed in a manner such that the reaction products accumulate on one side of the nanomotor, then diffusiophoresis may be responsible for propulsion. A model developed by Golestanian et al. [49], consists of a spherical structure with a point catalyst as shown in Fig. 10 marked “enzymatic site”. In this model, the reaction products that have accumulated at the catalyst site begin to diffuse away from the location of higher reaction product concentration driving the sphere away from this location as well. Since the sphere is constantly generating this concentration gradient, it is continually being propelled away from its catalyst site. The movement away from the catalyst has been verified [40–41]. This mechanism explains how a catalytic nanomotor is propelled away from the catalyst site as well, but another mechanism has been proposed to explain the same phenomenon.

### 3.2 Bubble propulsion

Autonomous movement of macroscopic plates was proposed to move by the impulse of bubble generated at the Pt catalysts site shown in Fig. 11 [42]. Plate movement as the result of bubble formation and eruption were clearly observed because the plates were large and floated along an aqueous  $\text{H}_2\text{O}_2$  solution. Ni/Au nanorods grown by TDEP were shown to be propelled by bubble propulsion as well [1]. Figure 12 shows a sequence of microscope images

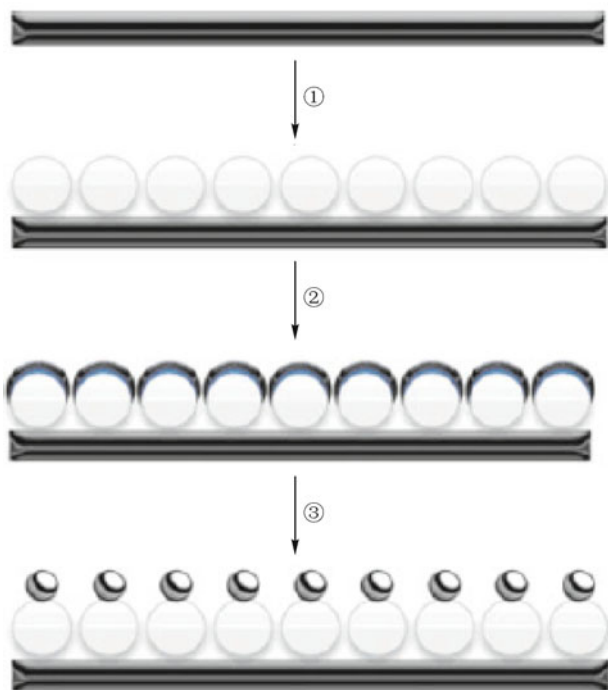


**Fig. 9** Fabrication of Pt-SiO<sub>2</sub> self-propelled dimers. First a monolayer of SiO<sub>2</sub> microbeads is placed onto a substrate; then a Cr adhesion layer is deposited followed by Pt; lastly, the structures are annealed at 900°C and then suspended into water by sonication. (Reproduced with permission from Ref. [45], Copyright 2010 WILEY-VCH Verlag GmbH & Co. KGaA, Weinheim)

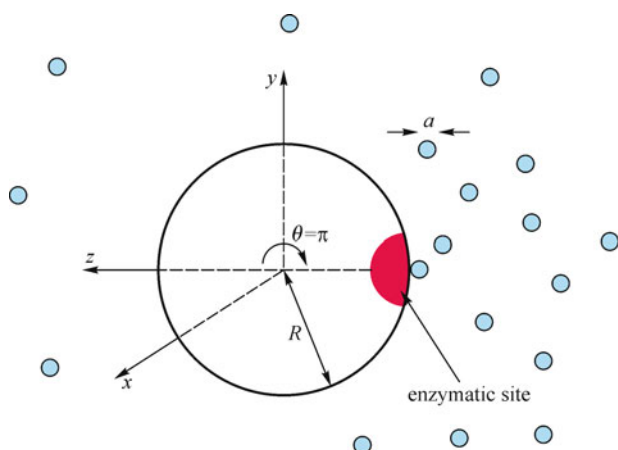


**Fig. 10** A schematic of the diffusiophoresis model in which a sphere with a single point catalyst site generates a concentration gradient of reaction products, driving the sphere away from this location. (Reproduced with permission from Ref. [49], Copyright 2005 The American Physical Society)

illuminating the jet of nanobubbles emanating from the Ni catalyst [1]. Bubble jets are clearly shown to propel rolled-up nanojet engines as bubbles are ejected from one side of the tube while H<sub>2</sub>O<sub>2</sub> fuel enters into the other side [35].

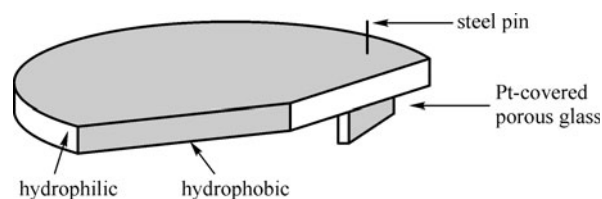


**Fig. 11** Autonomous swimming plates that have alternating hydrophilic-hydrophobic sides which induce self-assembly. The Pt coated on one side drives the plates across the aqueous solution of H<sub>2</sub>O<sub>2</sub> by bubble impulse. (Reproduced with permission from Ref. [42], Copyright 2002 WILEY-VCH Verlag GmbH, Weinheim, Fed. Rep. of Germany)

Physical models to explain how bubble propulsion is responsible for autonomous motion have been presented in the literature as well. One model explains how the mass change of O<sub>2</sub> bubbles detaching from the surface of a Pt-coated SiO<sub>2</sub> Janus sphere drives the particle and also relates bubble formation and the connection of surface tension

$$v \propto \gamma^2 \frac{kac}{1+ac} \quad (1)$$

where  $\gamma$ ,  $a$ , and  $c$  are surface tension, the Langmuir adsorption constant, and concentration, respectively [31]. Direct observations of bubbles coming from the surface, observations of nanomotors moving away from the stream of bubbles, and movement away from the catalyst makes a convincing argument that this model is correct for the particular nanomotor studied; however, there are other examples of nanomotors moving toward the catalyst which implies other forces are working on these structures.

### 3.3 Interfacial tension induced motion

An interfacial tension model is proposed to explain the movement of Au/Pt nanorod nanomotors fabricated by TDEP, and explains how this structure moves toward the Pt catalyst [22]. The Pt catalyst creates an interfacial tension gradient due to the larger quantity of O<sub>2</sub> near the Pt side of the nanomotor. This difference in surface tension is a function of the amount of O<sub>2</sub> generated which is proportional to the concentration of H<sub>2</sub>O<sub>2</sub> of the solution. The model suggests that the velocity,  $v$ , is linearly proportional to the surface tension of the solution and this corresponds well to the experimental data

$$v \propto \frac{SR^2\gamma}{\mu DL} \quad (2)$$

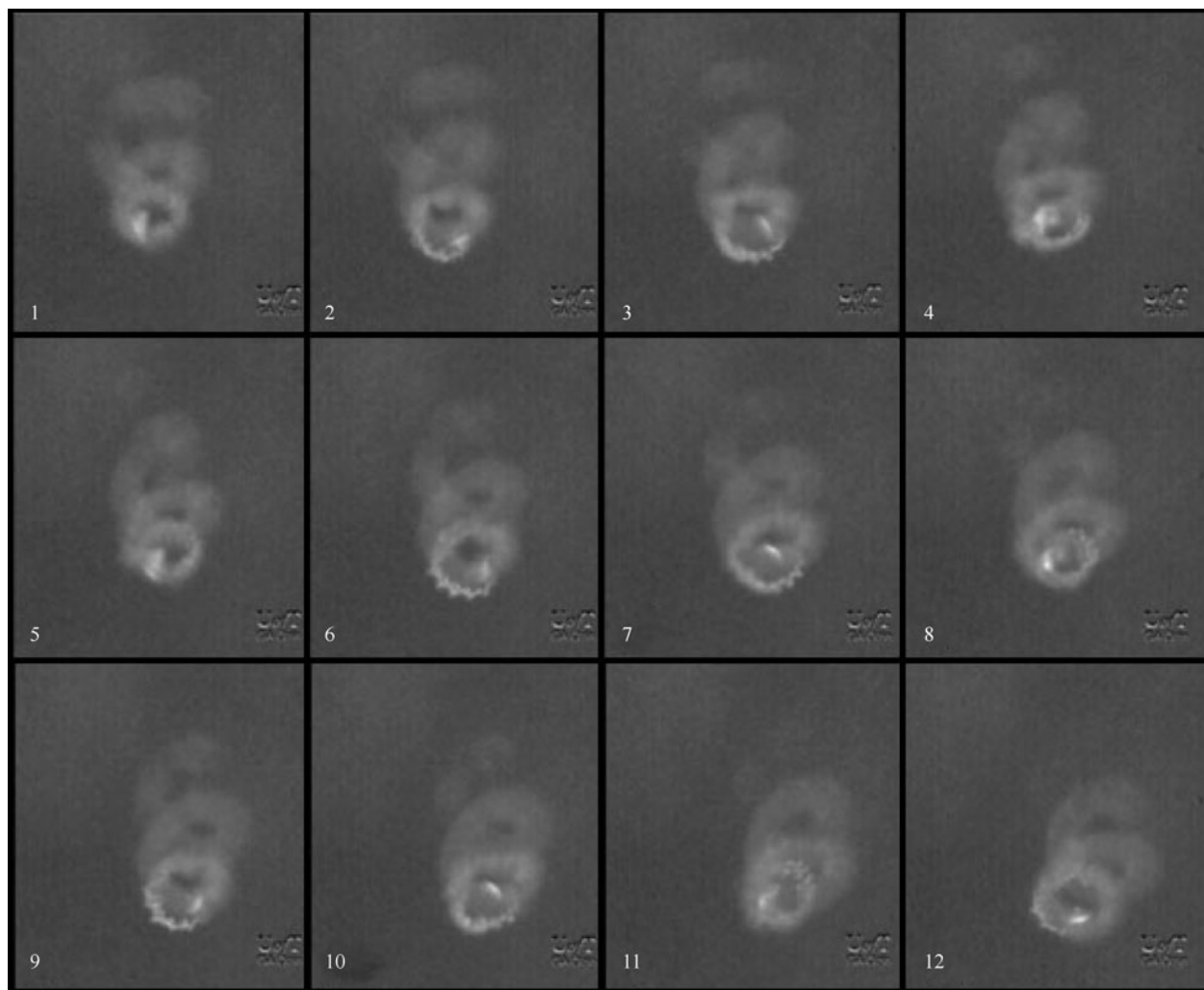


**Fig. 12** Micrograph images of a jet of nanobubbles coming from a spinning Au/Ni nanorod nanomotor. (Reproduced with permission from Ref. [1], Copyright 2005 WILEY-VCH Verlag GmbH & Co. KGaA, Weinheim)

where  $S$ ,  $R$ ,  $\gamma$ ,  $\mu$ ,  $D$ , and  $L$  are oxygen evolution rate, nanorod radius, surface tension, viscosity, diffusion coefficient, and nanorod length, respectively. This model not only predicts the correct direction of motion but also predicts the correct magnitude of force. Although successful, this model has a strong competitor which also accurately depicts the movement of bimetallic structures toward the catalyst, and this model is electrochemical by nature, and is known as self-electrophoresis.

### 3.4 Self-electrophoresis

When a catalytic nanomotor consists of two contacting metals, each metal can act as an electrode with one acting as a cathode and the other as an anode in the catalytic break-down of  $\text{H}_2\text{O}_2$ . The driving force for this type of catalytic nanomotor has been shown to be electrochemical

by nature, and a bipolar electrochemical model for nanorod nanomotors consisting of Au and Pt ends was first proposed by Paxton and Sen et al. [4,48]. Figure 13 shows the model of an Au/Pt nanorod nanomotor in which oxidation occurs at the Pt anode and reduction at the Au cathode for the overall reaction of  $\text{H}_2\text{O}_2 \rightarrow \text{H}_2\text{O} + \text{O}_2$  [48]. As shown in Fig. 10 the protons migrate from the Pt end to the Au end to recombine with the electrons, and in this process, the nanorod moves in the opposite direction, i.e., toward the Pt end. A scaling analysis for bimetallic nanorod structures gives an expression for nanomotor velocity as

$$u \propto \frac{\zeta F h \lambda_D j}{\eta D_+} \quad (3)$$

in which  $\zeta$ ,  $F$ ,  $h$ ,  $\lambda_D$ ,  $\eta$ ,  $D_+$ , and  $j$  are surface charge, Faraday constant, nanomotor length, Debye thickness,

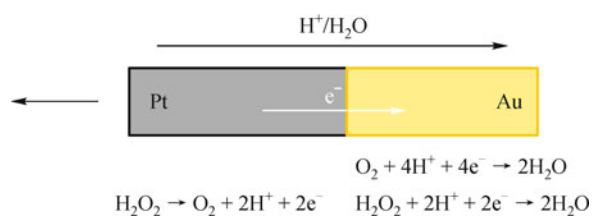


**Fig. 13** Schematic of the self-electrophoresis model in which the protons generated at the Pt end migrate to the Au end and in the process the nanorod structure moves toward the Pt end. (Reproduced with permission from Ref. [48], Copyright 2006 American Chemical Society)

viscosity, diffusion coefficient of protons, and the reaction flux, respectively [50]. This model has been used to predict convective flow induced by propelled micro tracer particles in a catalytic micropump [51]. In this system, an Ag island is placed in the middle of an Au substrate. The electroosmotic flow causes the particles to be pumped in a tight convection roll close to the Ag.

#### 4 Nanomotor motion control and applications

Catalytic nanomotors that move autonomously are appealing due to their lack of need of external influence. However, augmented control of autonomous nanomotors has been accomplished through various techniques, and control is leading to advances in practical applications for this field. Here we outline some of the examples of nanomotor manipulation and control. Using an external field is a simple method for controlling the direction of swimming motion. The incorporation of magnetic materials into Au/Pt nanorod nanomotors allowed for the remote-control of the swimming behaviors [27]. As an example, a

two Ni sections were added to the structure which swims autonomously in the presence of  $H_2O_2$ , but can be directed with an external magnetic field which aligns with the magnetized Ni sections. The Ni section is easily added using TDEP method. Solovev et al. incorporated a ferromagnetic layer of Fe/Co into their microtubular jet engines to allow for magnetic manipulation as well [35]. The incorporation of a Ni section allows for the guidance of nanorod nanomotors in a way so that they can perform certain tasks such as pick up and deliver cargo. Sen et al. assembled Au/Pt/PPy nanorod nanomotors to silica microspheres by electrostatic forces [44]. The Ni allowed for guidance of the nanomotor toward the cargo. The oppositely charged microsphere and PPy section of the nanorod made the attachment of the two possible. A similar example was presented by Wang et al. which involved a nanomotor picking up and moving a magnetic micro-particle cargo through a microchannel as shown in Fig. 14 [52]. The magnetic properties of an Au/Ni/Au/Pt-CNT nanorod nanomotor allowed for the pickup and release of the magnetic cargo. Non-catalytic, magnetic systems have been presented as well. Spiral shaped corkscrew motors grown by glancing angle deposition (GLAD) were powered solely by an external alternating magnetic field [53]. Figure 15(a) shows a cross section SEM of an array of these motors, and Fig. 15(b) shows an individual structure which clearly shows the microbead head and the spiral oxide layer. A thin layer of Co was deposited onto the structure after being removed from the surface, and then it was magnetized so that the magnetic moment was perpendicular to the long-axis. The external applied magnetic field controlled the movement in a precise manner. Flexible Au/Ag/Ni nanowires have been shown to swim in a rotating magnetic field [54]. In this example, the nanomotor has an Au head and a Ni tail which is linked

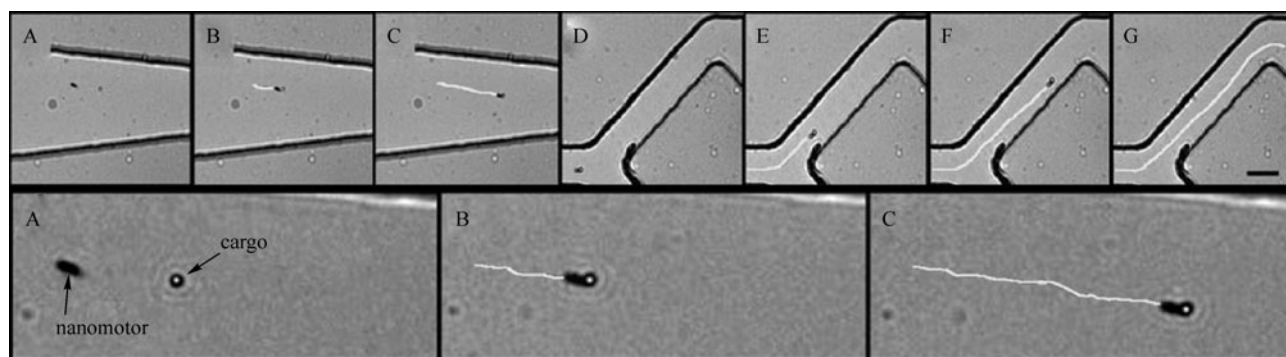


**Fig. 14** Shown in A–C, the loading of a magnetic microparticle cargo with an Au/Ni/Au/Pt-CNT nanomotor; Transportation of cargo through a PDMS microchannel is shown in D–G. (Reproduced with permission from Ref. [52], Copyright 2008 American Chemical Society)

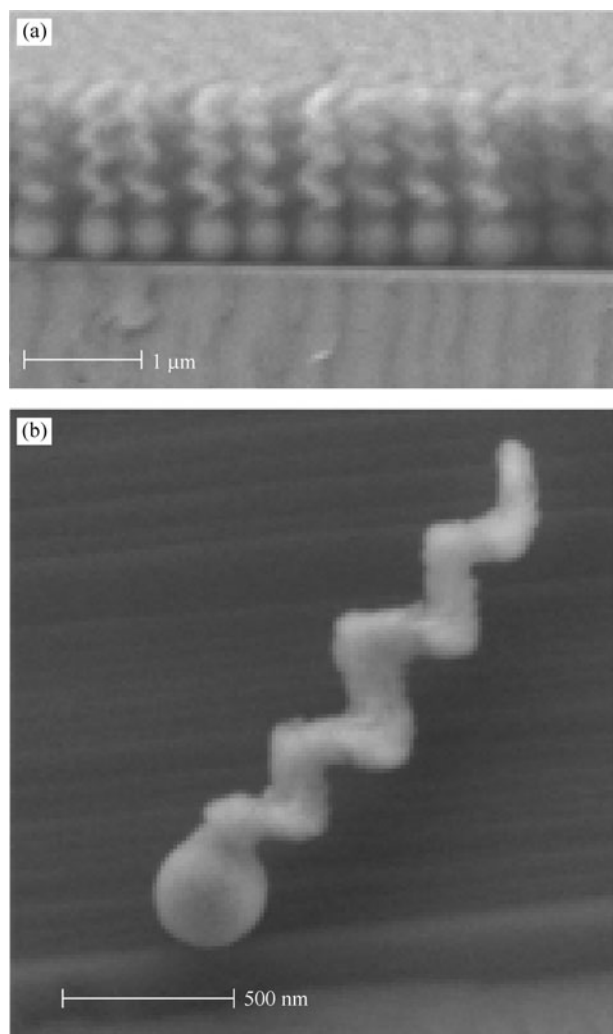


**Fig. 15** (a) Cross section SEM image and (b) individual magnetically controlled helical propeller grown by GLAD. (Reproduced with permission from Ref. [53], Copyright 2009 American Chemical Society)

by a partially dissolved and weakened bridge that is flexible. In the magnetic field, the tail moves back and forth causing the motor to swim. The use of magnetic materials combined with external magnetic fields is clearly an effective way to control and manipulate nanomotors, but other methods of control exist as well.

For the self-electrophoresis mechanism, altering the reaction leads to motion modulation. One interesting example is a thermally controlled catalytic nanomotor [55]. The speeds of this autonomous Au/Pt nanorod nanomotor are modulated by changing the temperature of the surrounding solution. Higher temperatures correspond to thermal activation of the redox reactions and therefore higher nanomotor velocities as is shown in Fig. 16. Ultimately, the self-electrophoresis mechanism is

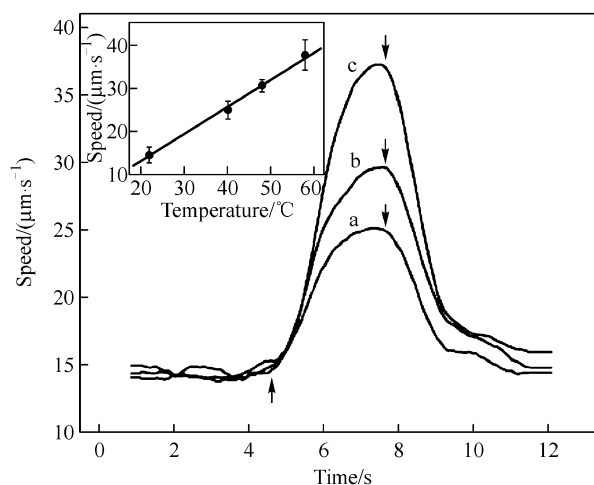


**Fig. 16** Thermally modulated speed versus time for Au/Pt nanorod nanomotor: three different heat pulses a, b, and c respectively corresponding to temperature 40°C, 48°C, and 58°C starting around 5 s and ending around 8 s. The inset graph shows a linear relationship between the speed and temperature. (Reproduced with permission from Ref. [55], Copyright 2009 Wiley-VCH Verlag GmbH & Co. KGaA, Weinheim)

responsible for the motion of this motor; the temperature only alters the potential difference between the two ends of the nanomotor altering the speed. Similarly, another way to increase the difference between the mixed potentials is to use a catalytic alloy [56]. By incorporating Ag into the Au section of an Au/Pt nanorod nanomotor, speeds are drastically increased showing a marked dependence upon nanomotor composition. The increase in speed is shown as a function of the percentage of Ag incorporated into the Au section of the nanorod in Fig. 17, showing a significant increase in speed with greater amounts of Ag. The addition of carbon nanotubes (CNT) to the Pt catalyst in an Au/Pt nanorod nanomotor also drastically increased the nanomotor speed [23]. By observing their speeds, catalytic nanomotors have recently been used to act as sensors for the presence of DNA and bacterial rRNA [57]. This example is an advanced application showing that biodetection is possible by simply observing speeds and distances traveled by catalytic nanomotors, and opens a new door for simple biodetection.

## 5 Conclusions

The field of catalytic nanomotors has rapidly developed in its short history. With the recent advances and the excellent contributions to this field, the future is bright. Some major current challenges exist and without a doubt, unforeseen

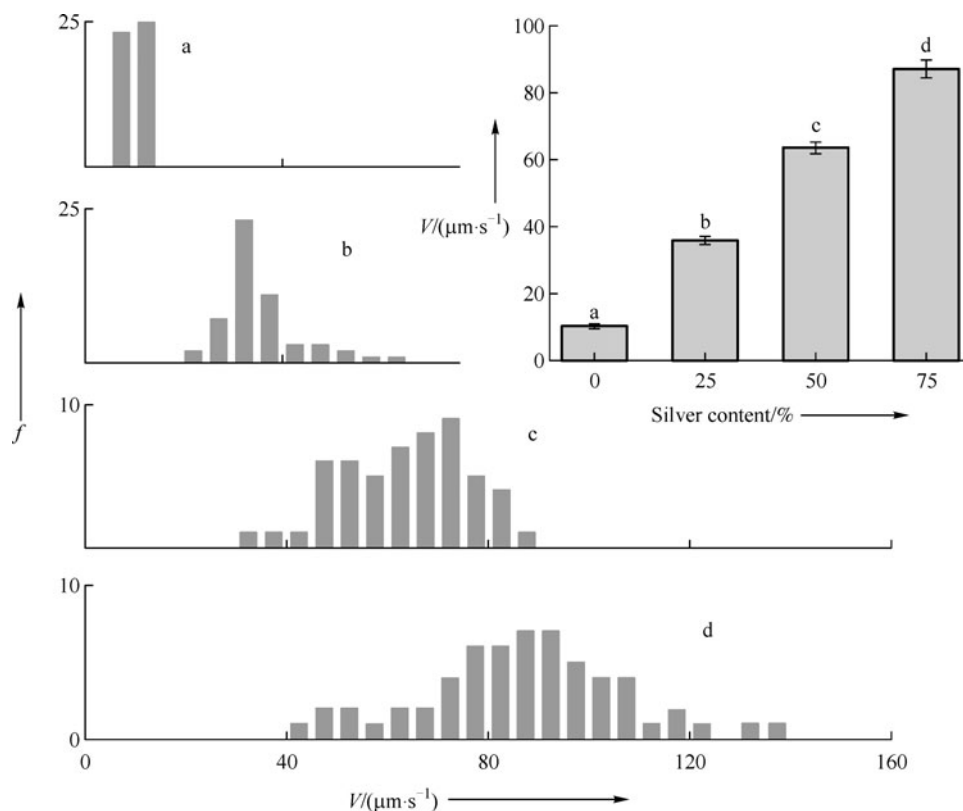


**Fig. 17** Speeds for various Ag contents of Au/Pt nanorod nanomotors: a, b, c, and d correspond to 0%, 25%, 50%, and 75% Ag in the Au section, respectively. (Reproduced with permission from Ref. [56], Copyright 2008 WILEY-VCH Verlag GmbH & Co. KGaA, Weinheim)

challenges remain veiled. The fabrication of functional nanomachines will require a culmination of all research avenues that have been discussed here as well as new innovations. Fabricating machines with individual parts, making nanomachines smart, and precisely controlling nanomachines are difficult yet exciting challenges. By gaining a complete understanding of the physical and chemical mechanisms involved, better control will be within reach and in the future, an industry of functional nanomachinery will be realized.

**Acknowledgements** We acknowledge the financial support from the National Science Foundation under Contract No. CMMI-0726770 and ECCS-0901141.

## References

- [1] Ozin G A, Manners I, Fournier-Bidoz S, et al. Dream nanomachines. *Advanced Materials*, 2005, 17(24): 3011–3018
- [2] Mirkovic T, Zacharia N S, Scholes G D, et al. Nanolocomotion-catalytic nanomotors and nanorotors. *Small*, 2010, 6(2): 159–167
- [3] Mirkovic T, Zacharia N S, Scholes G D, et al. Fuel for thought: chemically powered nanomotors out-swim nature's flagellated bacteria. *ACS Nano*, 2010, 4(4): 1782–1789
- [4] Paxton W F, Sen A, Mallouk T E. Motility of catalytic nanoparticles through self-generated forces. *Chemistry- a European Journal*, 2005, 11(22): 6462–6470
- [5] Paxton W F, Sundararajan S, Mallouk T E, et al. Chemical locomotion. *Angewandte Chemie*, 2006, 45(33): 5420–5429
- [6] Wang J. Can man-made nanomachines compete with nature biomotors? *ACS Nano*, 2009, 3(1): 4–9
- [7] Wang J, Manesh K M. Motion control at the nanoscale. *Small*, 2010, 6(3): 338–345
- [8] Schliwa M, Woehlke G. Molecular motors. *Nature*, 2003, 422 (6933): 759–765
- [9] Gajewski E, Steckler D K, Goldberg R N. Thermodynamics of the hydrolysis of adenosine 5'-triphosphate to adenosine 5'-diphosphate. *The Journal of Biological Chemistry*, 1986, 261(27): 12733–12737
- [10] Alberts B, Johnson A, Lewis J, et al. *Molecular Biology of the Cell*. 4th ed. New York: Garland Science, 2002
- [11] Kron S J, Spudich J A. Fluorescent actin filaments move on myosin fixed to a glass surface. *Proceedings of the National Academy of Sciences of the United States of America*, 1986, 83 (17): 6272–6276
- [12] Browne W R, Feringa B L. Making molecular machines work.

- Nature Nanotechnology, 2006, 1(1): 25–35
- [13] Kay E R, Leigh D A, Zerbetto F. Synthetic molecular motors and mechanical machines. *Angewandte Chemie*, 2007, 46(1–2): 72–191
- [14] Kinbara K, Aida T. Toward intelligent molecular machines: directed motions of biological and artificial molecules and assemblies. *Chemical Reviews*, 2005, 105(4): 1377–1400
- [15] Cameron L A, Footer M J, van Oudenaarden A, et al. Motility of ActA protein-coated microspheres driven by actin polymerization. *Proceedings of the National Academy of Sciences of the United States of America*, 1999, 96(9): 4908–4913
- [16] Soong R K, Bachand G D, Neves H P, et al. Powering an inorganic nanodevice with a biomolecular motor. *Science*, 2000, 290(5496): 1555–1558
- [17] Mano N, Heller A. Bioelectrochemical propulsion. *Journal of the American Chemical Society*, 2005, 127(33): 11574–11575
- [18] Sanchez S, Solovev A A, Mei Y, et al. Dynamics of biocatalytic microengines mediated by variable friction control. *Journal of the American Chemical Society*, 2010, 132(38): 13144–13145
- [19] Pantarotto D, Browne W R, Feringa B L. Autonomous propulsion of carbon nanotubes powered by a multienzyme ensemble. *Chemical Communications*, 2008, (13): 1533–1535
- [20] Ebbens S J, Howse J R. In pursuit of propulsion at the nanoscale. *Soft Matter*, 2010, 6(4): 726–738
- [21] Nicewarner-Pena S R, Freeman R G, Reiss B D, et al. Submicrometer metallic barcodes. *Science*, 2001, 294(5540): 137–141
- [22] Paxton W F, Kistler K C, Olmeda C C, et al. Catalytic nanomotors: autonomous movement of striped nanorods. *Journal of the American Chemical Society*, 2004, 126(41): 13424–13431
- [23] Laocharoensuk R, Burdick J, Wang J. Carbon-nanotube-induced acceleration of catalytic nanomotors. *ACS Nano*, 2008, 2(5): 1069–1075
- [24] Qin L D, Banholzer M J, Xu X, et al. Rational design and synthesis of catalytically driven nanorotors. *Journal of the American Chemical Society*, 2007, 129(48): 14870–14871
- [25] Manesh K M, Cardona M, Yuan R, et al. Template-assisted fabrication of salt-independent catalytic tubular microengines. *ACS Nano*, 2010, 4(4): 1799–1804
- [26] Catchmark J M, Subramanian S, Sen A. Directed rotational motion of microscale objects using interfacial tension gradients continually generated via catalytic reactions. *Small*, 2005, 1(2): 202–206
- [27] Kline T R, Paxton W F, Mallouk T E, et al. Catalytic nanomotors: remote-controlled autonomous movement of striped metallic nanorods. *Angewandte Chemie*, 2005, 44(5): 744–746
- [28] Love J C, Gates B D, Wolfe D B, et al. Fabrication and wetting properties of metallic half-shells with submicron diameters. *Nano Letters*, 2002, 2(8): 891–894
- [29] Golestanian R, Liverpool T B, Ajdari A. Designing phoretic micro- and nano-swimmers. *New Journal of Physics*, 2007, 9: 126 (9 pages)
- [30] Howse J R, Jones R A, Ryan A J, et al. Self-motile colloidal particles: from directed propulsion to random walk. *Physical Review Letters*, 2007, 99(4): 048102 (4 pages)
- [31] Gibbs J G, Zhao Y P. Autonomously motile catalytic nanomotors by bubble propulsion. *Applied Physics Letters*, 2009, 94(16): 163104 (3 pages)
- [32] Wheat P M, Marine N A, Moran J L, et al. Rapid fabrication of bimetallic spherical motors. *Langmuir*, 2010, 26(16): 13052–13055
- [33] Gibbs J G, Fragnito N A, Zhao Y P. Asymmetric Pt/Au coated catalytic micromotors fabricated by dynamic shadowing growth. *Applied Physics Letters*, 2010, 97: 253107 (3 pages)
- [34] Wang Y, Fei S T, Byun Y M, et al. Dynamic interactions between fast microscale rotors. *Journal of the American Chemical Society*, 2009, 131(29): 9926–9927
- [35] Solovev A A, Mei Y, Bermúdez Ureña E, et al. Catalytic microtubular jet engines self-propelled by accumulated gas bubbles. *Small*, 2009, 5(14): 1688–1692
- [36] Robbie K, Brett M J. Sculptured thin films and glancing angle deposition: Growth mechanics and applications. *Journal of Vacuum Science & Technology A: Vacuum, Surfaces, and Films*, 1997, 15(3): 1460–1465
- [37] Robbie K, Brett M J, Lakhtakia A. Chiral sculptured thin films. *Nature*, 1996, 384(6610): 616
- [38] Zhao Y P, Ye D X, Wang P I, et al. Fabrication of Si nanocolumns and Si square spirals on self-assembled monolayer colloid substrates. *International Journal of Nanoscience*, 2002, 1(1): 87–97
- [39] Zhao Y P, Ye D X, Wang G C, et al. Novel nano-column and nano-flower arrays by glancing angle deposition. *Nano Letters*, 2002, 2(4): 351–354
- [40] He Y P, Wu J S, Zhao Y P. Designing catalytic nanomotors by dynamic shadowing growth. *Nano Letters*, 2007, 7(5): 1369–1375
- [41] Gibbs J G, Zhao Y P. Design and characterization of rotational multicomponent catalytic nanomotors. *Small*, 2009, 5(20): 2304–2308
- [42] Ismagilov R F, Schwartz A, Bowden N, et al. Autonomous movement and self-assembly. *Angewandte Chemie*, 2002, 114(4): 674–676
- [43] Mirkovic T, Foo M L, Arsenaault A C, et al. Hinged nanorods made using a chemical approach to flexible nanostructures. *Nature Nanotechnology*, 2007, 2(9): 565–569
- [44] Sundararajan S, Lammert P E, Zudans A W, et al. Catalytic motors for transport of colloidal cargo. *Nano Letters*, 2008, 8(5): 1271–

1276

- [45] Valadares L F, Tao Y G, Zacharia N S, et al. Catalytic nanomotors: self-propelled sphere dimers. *Small*, 2010, 6(4): 565–572
- [46] Ebbens S, Jones R A L, Ryan A J, et al. Self-assembled autonomous runners and tumblers. *Physical Review E: Statistical, Nonlinear, and Soft Matter Physics*, 2010, 82(2): 015304 (4 pages)
- [47] Gibbs J G, Zhao Y P. Self-organized multiconstituent catalytic nanomotors. *Small*, 2010, 6(15): 1656–1662
- [48] Wang Y, Hernandez R M, Bartlett D J Jr, et al. Bipolar electrochemical mechanism for the propulsion of catalytic nanomotors in hydrogen peroxide solutions. *Langmuir*, 2006, 22(25): 10451–10456
- [49] Golestanian R, Liverpool T B, Ajdari A. Propulsion of a molecular machine by asymmetric distribution of reaction products. *Physical Review Letters*, 2005, 94(22): 220801 (4 pages)
- [50] Moran J L, Wheat P M, Posner J D. Locomotion of electrocatalytic nanomotors due to reaction induced charge autoelectrophoresis. *Physical Review E: Statistical, Nonlinear, and Soft Matter Physics*, 2010, 81(6): 065302 (4 pages)
- [51] Kline T R, Paxton W F, Wang Y, et al. Catalytic micropumps: microscopic convective fluid flow and pattern formation. *Journal of the American Chemical Society*, 2005, 127(49): 17150–17151
- [52] Burdick J, Laocharoensuk R, Wheat P M, et al. Synthetic nanomotors in microchannel networks: directional microchip motion and controlled manipulation of cargo. *Journal of the American Chemical Society*, 2008, 130(26): 8164–8165
- [53] Ghosh A, Fischer P. Controlled propulsion of artificial magnetic nanostructured propellers. *Nano Letters*, 2009, 9(6): 2243–2245
- [54] Gao W, Sattayasamitsathit S, Manesh K M, et al. Magnetically powered flexible metal nanowire motors. *Journal of the American Chemical Society*, 2010, 132(41): 14403–14405
- [55] Balasubramanian S, Kagan D, Manesh K M, et al. Thermal modulation of nanomotor movement. *Small*, 2009, 5(13): 1569–1574
- [56] Demirok U K, Laocharoensuk R, Manesh K M, et al. Ultrafast catalytic alloy nanomotors. *Angewandte Chemie*, 2008, 120(48): 9489–9491
- [57] Wu J, Balasubramanian S, Kagan D, et al. Motion-based DNA detection using catalytic nanomotors. *Nature Communications*, 2010, 1: 36